RESEARCH ARTICLE

Down-regulation of miR-377 suppresses high glucose and hypoxia-induced angiogenesis and inflammation in human retinal endothelial cells by direct up-regulation of target gene SIRT1

Chunmei Cui[1] · Yuehua Li[1] · Ying Liu[1]

Abstract

Diabetic retinopathy (DR) is one of the common microvascular complications of diabetes mellitus, which is the main cause of blindness in diabetic patients. Angiogenesis plays an important role in retinal detachment and retinal microvascular inflammation throughout the whole development of DR. This study aimed to investigate the regulatory effect and the potential mechanism of miR-377 on high glucose and hypoxia-induced angiogenesis and inflammation in human retinal endothelial cells, and found that the miR-377 level was significantly increased after high glucose and hypoxia-mimetic agent to simulate the DR milieu. Moreover, miR-377 was confirmed to directly decrease target SIRT1 gene, further aggravated proliferation, cell cycle transition, migration and angiogenesis, pro-inflammatory molecules release induced by high glucose and hypoxia in vitro. Conversely, down-regulation of miR-377 enhanced expression of SIRT1 and in turn alleviated high glucose and hypoxia-induced angiogenesis and inflammation in vitro. Additionally, Western blot results showed that down-regulation of miR-377 restrained high glucose and hypoxia-induced protein expressions of p-IκBα, nuclear P65 and p-P65. Conversely, up-regulation of miR-377 presented opposite results. Conclusively, down-regulation of miR-377 could partially suppress high glucose and hypoxia-induced angiogenic functions, restrain pro-inflammatory cytokines release, and its mechanism may though inhibition of NF-κB pathway by direct up-regulation of target gene SIRT1 expression. Our study suggests that miR-377 may be used as a potential novel target for prevention strategy for DR.

Keywords MiR-377 · Human retinal endothelial cell · Angiogenesis · Inflammatory response · Diabetic retinopathy

Introduction

Diabetes mellitus (DM) is the most common but seriously endangering human health chronic metabolic disease caused by multiple factors. As reported, the incidence of DM in China is about 10.9% at present, however, the incidence is on the rise due to changes of diet [1]. And diabetic retinopathy (DR) is one of the common microvascular complications of DM patients, which is the main cause of blindness in DM

patients [2]. In recent years, due to the increasing number of DM patients, the incidence of DR has also increased rapidly [3]. Although the research on prevention and treatment of DR has made some achievements in recent years, however, the treatment of DR still fails to achieve satisfactory results. Although the commonly used drugs such as hypertension, lipid-lowering and glucose-lowering can control the progress of DR to some extent, it is undeniable that these drugs cannot completely reverse the occurrence and development of DR [4, 5]. Although retinal photocoagulation and intravitreal injection have achieved certain therapeutic effects, the visual function of DR patients cannot be completely repaired, and the problem of high wound infection and recurrence rate has not been solved [6]. The pathological changes and pathogenesis of DR involve the co-action of multiple gene and multiple signaling pathways. Currently, the pathogenesis of DR involves angiogenesis, oxidative stress, chronic inflammation, and etc [7]. Neovascularization on the surface of the retina, is a key stage of proliferative DR, and it is also one of

✉ Chunmei Cui
chunmeicui@yeah.net

1 Department of Ophthalmology, Beijing Chaoyang Hospital, Capital Medical University, No. 8 Gongti South Road, Chaoyang District, Beijing 100020, China

the important factors of retinal detachment [8]. In addition, long-term chronic hyperglycemia and hypoxia microenvironment induced retinal microvascular inflammation throughout the whole development of DR [9]. Therefore, it is of great significance to study the mechanism of angiogenesis and inflammation of human retinal endothelial cells induced by high glucose and hypoxia for the prevention and treatment of DR.

MicroRNAs (miRNAs) are a type of highly conserved, non-coding and single-stranded RNAs with 18–25 nucleotides lengths, which can regulate the expression of target genes at post-transcriptional level [10]. MiRNAs are involved in almost all pathological and physiological processes of the body, including cell proliferation [11], differentiation [12], immune inflammation [13], migration [14] and apoptosis [15]. Moreover, increasing studies demonstrated that miRNAs have been gradually emerged as important regulators of angiogenesis and involved in various aspects of DR [16]. Many valuable miRNAs such as miR-181a [17], miR-21 [18] and miR-15a [19] have been found to be play important roles in DR. However, many miRNAs involved in the regulation of the development of DR have not been explored. MiR-377 is derived from DLK1-DIO3 gene cluster, and previous studies about its function are focused on tumor-related diseases [20]. Recent studies have demonstrated that the expression of miR-377 was significantly higher in diabetic nephropathy [21]. However, the functional role of miR-377 in HRECs after high glucose and hypoxia-mimetic agent to simulate the diabetic retinopathy milieu remains unknown.

In this study, we first found that the miR-377 level was significantly increased after high glucose and hypoxia-mimetic agent to simulate the diabetic retinopathy milieu. Indeed, miR-377 was confirmed to directly decrease target SIRT1 gene, further aggravated proliferation, cell cycle transition, migration and angiogenesis, inflammatory molecules release induced by high glucose and hypoxia in vitro. Conversely, down-regulation of miR-377 enhanced expression of SIRT1 and in turn alleviated high glucose and hypoxia-induced angiogenesis and inflammation in vitro. In short, miR-377 may be used as a potential novel target for prevention strategy for DR.

Materials and methods

Cell culture

HRECs were purchased from ScienCell Research Laboratories (San Diego, CA, USA). And the cells were maintained in Endothelial Cell (EC) Medium (ScienCell, San Diego, CA, USA) supplemented with 10% fetal bovine serum (FBS) (Hyclone, South Logan, UT, USA), 100 U/mL penicillin–streptomycin (Invitrogen, Carlsbad, CA, USA) and 5 ng/mL endothelial cell growth factor (β-ECGF) (R&D Systems, Minneapolis, MN, USA) and incubated in a humidified atmosphere containing 5% CO_2 at 37 °C on 0.1% gelatin-coated culture flasks (Corning, NY, USA).

Transient transfection

The oligonucleotides miR-377 mimics (377-m), negative control miR mimic (NC-m), miR-377 inhibitor (377-i), negative control miR inhibitor (NC-i), siRNA for SIRT1 (si-SIRT1), siRNA-negative control (si-NC) were purchased from GenePharma (Pudong, Shanghai, China). The SIRT1-overexpression plasmid was synthesized by inserting full-length SIRT1 cDNA sequences into a pcDNA3.1-vector and sequenced confirmed by RiboBio (Guangzhou, Guangdong, China). HRECs were transfected with 377-m, 377-i, si-SIRT1 and pcDNA3.1-SIRT1 according to the manufacturer's instructions. Briefly, HRECs confluence reached about 60%, the cells were changed to the FBS-free and antibiotic-free medium and synchronised for 12 h. Then, Lipofectamine^{TM}2000 reagent (Invitrogen, Carlsbad, CA, USA) was applied to assist the transfection of 377-m, 377-i, si-SIRT1 and pcDNA3.1-SIRT1 at a final dose of 50 nM in the static state. After incubation for 8 h at 37 °C, the cells were changed back to fresh EC medium supplemented with 10% FBS, 100 U/mL penicillin–streptomycin and 5 ng/mL β-ECGF. Followed, the cells were re-cultured for 48 h. After confirmed the transfection efficiency by qRT-PCR analysis or Western blot analysis, the cells were used for the following study.

Cell proliferation assay

Cell proliferation was measured using Cell Counting Kit-8 (CCK-8) (Dojindo, Kumamoto, Japan) assay and 5-bromo-2-deoxyuridine (Brdu) colorimetric assay kit (Roche, Basel, Switzerland) according to the manufacturer's instructions. Briefly, HRECs in logarithmic growth phase were seeded in 96-well plate at a final cell density of 5.0×10^4 cells/mL. For CCK-8 assay, after indicated treatment for 24, 48 or 72 h, the cells were incubated with 10 μL CCK-8 reagent solution at 37 °C for 2 h, then measured the optical density (OD) value at wavelength of 450 nm with a microplate reader(Bio-Tek Elx800, Winooski, VT, USA). For Brdu assay, after indicated treatment for 24, 48 or 72 h, the cells were incubated with 10 μL Brdu labeling reagent solution at 37 °C for 2 h. Then, the labeling medium was removed and incubated with 100 μL FixDenat reagent solution at room temperature for 30 min. Followed, FixDenat solution was removed and incubated with 100 μL anti-Brdu-POD solution at room temperature for 90 min. Followed, the anti-Brdu-POD solution was removed and rinsed the well with phosphate-buffered

saline (PBS) for three times. Substrate solution was added and incubated at room temperature for 15 min. Finally, the termination buffer was added to stop the reaction. The OD value of Brdu incorporation was measured at wavelength of 450 nm with a microplate reader (Bio-Tek Elx800, Winooski, VT, USA). Four complex holes were set for each group; meanwhile, single holes without cells were set as the blank control group. The mean OD value was obtained from three independent experiments. The relative growth rate (RGR) of HRECs was calculated as: RGR (%) = (OD value of treatment group − OD value of blank control)/(OD value of control group − OD value of blank control)×100%.

To simulate the diabetic retinopathy milieu model in vitro, HRECs were seeded in 96-well plate at a final cell density of 5.0×10^4 cells/mL and stimulated with various does (5.5, 11.0, 16.5, 22.0, 27.5, 33.0, 38.5 or 44.0 mmol/L) of D-glucose (Sigma, St. Louis, MO, USA), various does (9.5, 18.5, 37.5, 75.0, 150.0, 200.0 or 300.0 μmol/L) of hypoxia-mimetic agent (CoCl$_2$) (Sigma, St. Louis, MO, USA), or 30 mmol/L mannitol(Sigma, St. Louis, MO, USA) for different times(24, 48 or 72 h), respectively. As shown in Supplemental Fig. 1A–C, D-glucose at does of 27.5 mmol/L and CoCl$_2$ at does of 150.0 μmol/L for 48 h was the best method of the experimental condition, however, mannitol did not affect the growth rate of HRECs. We further examined the effect of high glucose (HG, 27.5 mmol/L D-glucose), hypoxia-mimetic agent (HY, 150 μmol/L CoCl$_2$), high mannitol (HM, 30 mmol/L mannitol), HG + HM, HY + HM or HG + HY on the growth rate of HRECs, respectively. As shown in Supplemental Fig. 1D, after treatment with HG, HM or HY for 48 h, HG or HY enhanced the growth rate of HRECs, and HG + HY further enhanced the growth rate of HRECs. The data suggested that HY and HG had a synergistic effect on cell growth in HRECs. Therefore, D-glucose at does of 27.5 mmol/L and CoCl$_2$ at does of 150.0 μmol/L for 48 h was selected as the best experimental condition for following experiments.

Cell cycle analysis

Cell cycle distribution was evaluated by propidium iodide (PI) (KeyGen, Nanjing, Jiangsu, China) staining according to the manufacturer's instructions. Briefly, HRECs were seeded in 6-well plate at a final cell density of 5.0×10^4 cells/mL. After indicated treatments for 48 h, HRECs were trypsinized, and then collected by centrifuged. The cells were re-suspended with ice-cold PBS for twice and then fixed with ice-cold 75% (v/v) ethanol for 24 h at 4 °C. Then cells were re-suspended with ice-cold PBS for twice. Finally, the cells were incubated PI reagent solution at room temperature for 30 min in the dark. The DNA content of each sample was determined using a CytoFLEX flow cytometry (Beckman, Miami, FL, USA). The percentages of cell count in different phases were quantified using a ModFit LT software (Verity Software House, USA).

Transwell assay

Cell migration was assayed using 24-well Transwell chambers with 6.5 mm diameter polycarbonate membrane (Corning, NY, USA) according to the manufacturer's instructions. Briefly, HRECs were seeded in the upper side of the chamber at a final cell density of 5.0×10^4 cells/mL with 100 μL FBS-free EC Medium supplemented with 0.2% BSA. The bottom side of the chamber was added 600 μL EC Medium supplemented with 10% FBS. After indicated treatments for 48 h, non-migrated cells of the upper side of polycarbonate membrane surface were removed. Migrated cells of the bottom side of polycarbonate membrane surface were fixed with 4% paraformaldehyde and stained with 0.5% crystal violet reagent solution. Migrated cells were quantified by counting cells using a ECLIPSE Ts2 inverted phase contrast microscopy (Nikon, Tokyo, Japan).

Wound healing assay

Wound healing assay was applied as described previously [22]. Briefly, HRECs were seeded in 24-well plate at a final cell density of 5.0×10^4 cells/mL. After indicated treatments for 48 h, when HRECs confluence reached about 100%, the confluent cell monolayer was scraped with a sterile 100 μL tip to make a scratch across the center of the circle. The wound areas of each sample were observed using a ECLIPSE Ts$_2$ inverted phase contrast microscopy (Nikon, Tokyo, Japan) and evaluated using a Image-Pro Plus 6.0 software (Media Cybernetics, Silver Springs, MD, USA) at 0 h and 48 h.

Tube formation assay

Tube formation assay was performed as described previously [23]. Briefly, the upper surfaces of the wells of 96-well plate were covered with matrigel (BD Biosciences, San Jose, CA, USA). HRECs were seeded in 96-well plate at a final cell density of 5.0×10^4 cells/mL in 100 μL EC medium supplemented with 10% FBS. After indicated treatments for 48 h, tube-like structures of each sample were observed using a ECLIPSE Ts2 inverted phase contrast microscopy (Nikon, Tokyo, Japan). Moreover, the percentages of total tubes formations were quantified using a Image-Pro Plus 6.0 software (Media Cybernetics, Silver Springs, MD, USA).

ELISA assay

The levels of TNF-α, IL-8, IL-6 and MCP-1 were evaluated using TNF-α, IL-8, IL-6 and MCP-1 ELISA kits

(R&D Systems, Minneapolis, MN, USA) according to the manufacturer's instructions, respectively. Briefly, HRECs were seeded in 96-well plate at a final cell density of 5.0×10^4 cells/mL in 100 μL EC medium supplemented with 10% FBS. After indicated treatments for 48 h, the conditioned medium of each sample was collected. TNF-α, IL-8, IL-6 and MCP-1 standards and the conditioned medium were added into wells overlayed with the appropriate antibodies. Then the HRP labeled streptomycin antibody was added into the wells and incubated at 37 °C for 90 min. Followed, the solution was removed and rinsed the well with PBS for 3 times. Moreover, substrate solution was added and incubated at 37 °C for 10 min. Finally, the termination buffer was added to stop the reaction. The OD values of TNF-α, IL-8, IL-6 and MCP-1 were measured at wavelength of 450 nm with a microplate reader (Bio-Tek Elx800, Winooski, VT, USA). The levels of TNF-α, IL-8, IL-6 and MCP-1 were calculated with the standard curve.

Quantitative reverse transcription PCR (qRT-PCR) assay

Total RNA of HRECs was isolated using a TRIzol™ reagent (Thermo Fisher Scientific, Waltham, MA, USA) according to the manufacturer's instructions. For miRNA assay, a TaqMan™ MicroRNA Reverse Transcription Kit (Thermo Fisher Scientific, Waltham, MA, USA) and a TaqMan™ MicroRNA Kit (Qiagen, Duesseldorf, Germany) were carried out with a ABI7300 real-time PCR system (Applied Biosystems, Waltham, MA, USA) according to the manufacturer's instructions. The level of miR-377 of each sample was normalized to U6 small nuclear RNA and quantified using the $2^{-\Delta\Delta CT}$ method. For mRNA assay, cDNA was synthesized using a Super Script III Reverse Transcriptase Kit (Invitrogen, Carlsbad, CA, USA) and the expressions of mRNAs were conducted using a SYBR Green PCR Kit (TaKaRa, Tokyo, Japan) according to the manufacturer's instructions. The levels of PCNA, Ki-67, cyclinD1, cyclinB, MMP-2, MMP-9, VEGF and SIRT1 of each sample were normalized to GAPDH and quantified using the $2-\Delta\Delta CT$ method. The used primers were listed in Supplemental Table 1.

Dual-luciferase reporter assay

The pGL3-SIRT1-3′UTR wild-type vector plasmid and pGL3-SIRT1-3′UTR mutant vector plasmid were synthesized by inserting 3′UTR wild-type or 3′UTR mutant of SIRT1 into the luciferase reporter pGL3-control vector and sequenced confirmed by GenePharma (Pudong, Shanghai, China). Briefly, HRECs were seeded in 24-well plate at a final cell density of 5.0×10^4 cells/mL. When the cell confluence reached about 60%, the cells were changed to the

FBS-free and antibiotic-free medium and synchronised for 12 h. Then the pGL3-SIRT1-3′UTR wild-type vector plasmid or mutant vector plasmid, 377-m, 377-i, NC-i, NC-m or pRL-TK Renilla luciferase reporter (Promega, Madison, WI, USA) were co-transfected into the cells using Lipofectamine 2000 (Invitrogen, Carlsbad, CA, USA). After co-incubated for 48 h, the luciferase and renilla activities were determined with a Dual-Luciferase Reporter Kit (Promega, Madison, WI, USA) according to the manufacturer's instructions.

Whole-cell, nuclear and cytoplasmic proteins isolation

Whole-cell proteins were isolated with a Total Protein Extraction Kit (Beyotime, Ningbo, Jiangsu, China) according to the manufacturer's instructions. Briefly, after indicated treatment, HRECs were harvested and incubated with 100 μL ice-cold RIPA solution at 4 °C for 30 min. Then the cells were centrifuged at $12,000 \times g$ for 10 min and the supernatant (whole-cell proteins) were collected for the following Western blot analysis.

Nuclear and cytoplasmic proteins were isolated with a Nuclear and Cytoplasmic Protein Extraction Kit (Invitrogen, Carlsbad, CA, USA) according to the manufacturer's instructions. Briefly, after indicated treatment, HRECs were harvested and incubated with 100 μL ice-cold CERI solution at 4 °C for 10 min. Then, the cells were incubated with 10 μL ice-cold CERII solution at 4 °C for 5 min and then centrifuged at $12,000 \times g$ for 5 min. The sediment was incubated with 50 μL ice-cold NER solution at 4 °C for 10 min and then centrifuged at $12,000 \times g$ for 12 min. At last, the supernatant (nuclear proteins) and the sediment (cytoplasmic proteins) were collected for the following Western blot analysis.

Western blot analysis

The proteins were extracted from whole-cell, nucleus and cytoplasm were performed to Western blot analysis as described previously [24]. Briefly, the protein concentration was quantified with a BCA Quantitative Detection Kit (Beyotime, Ningbo, Jiangsu, China), and equal amounts of protein (80 μg protein per sample) were size-fractionated electrophoretically using SDS–PAGE on 10% separation gels. And then the proteins were transferred onto PVDF membranes (Millipore, Billerica, MA, USA). After blocking with 5% non-fat milk, the membranes were loaded with primary antibodies including PCNA antibody, Ki-67 antibody, cyclinD1 antibody, cyclinB antibody, MMP-2 antibody, MMP-9 antibody, VEGF antibody, SIRT1 antibody, P65 antibody, p-IκBα antibody, IκBα antibody and β-actin antibody (1:1000 dilution; Santa Cruz, CA, USA) at 4 °C overnight. Then, the antibody solution was removed and

incubated with the secondary antibodies carrying HRP solution (1:1000 dilution; Beyotime, Ningbo, Jiangsu, China) at room temperature for 45 min. The proteins were visualized with a ECL Detection Kit (Beyotime, Ningbo, Jiangsu, China). β-actin was performed as an internal control. The density of the protein bands was quantified using a Image-Pro Plus 6.0 software (Media Cybernetics, Silver Springs, MD, USA).

Statistical analysis

All data of the study from three independent experiments were expressed as mean ± standard deviation (SD). Statistical analysis was performed by one-way analysis of variance (ANOVA) followed by Bonferroni multiple comparison post hoc test using a SPSS 19.0 software(SPSS Inc., Chicago, IL, USA). *P* values < 0.05 were considered to be statistically significant.

Results

Effect of miR-377 on high glucose and hypoxia-induced proliferation and cell cycle progression in HRECs

Cell proliferation plays an important role in the angiogenesis of DR [25]. To investigate the regulatory effect of miR-377 on high glucose and hypoxia-induced proliferation in HRECs, we first examined whether high glucose and hypoxia-induced proliferation in HRECs was correlated with the miR-377 expression. High glucose and hypoxia-induced proliferation in HRECs was evaluated by CCK-8 assay and Brdu assay, the endogenous miR-377 level was examined by qRT-PCR. As shown in Supplemental Fig. 2A–C, after stimulated the cells with 27.5 mmol/L D-glucose and 150.0 μmol/L CoCl$_2$ for 48 h, the cell viability and Brdu incorporation were significantly increased and parallel to a significant increased the miR-377 expression. The results suggested that miR-377 expression may be involved in high glucose and hypoxia-induced proliferation in HRECs. To explore the potential interaction between miR-377 expression and cell proliferation, we further investigated the regulatory effects of miR-377 knockdown by transfected with miR-377 inhibitor or miR-377 over-expression by transfected with miR-377 mimic on cell proliferation in HRECs. The miRNA transfection efficiency was evaluated by qRT-PCR assay. As shown in Supplemental Fig. 3, compared with control group, the level of miR-377 was significantly increased in the miR-377 mimic group, and decreased in miR-377 inhibitor group after transfection for 48 h. As shown in Fig. 1a, b, miR-377 knockdown significantly reduced the high glucose and hypoxia-induced cell viability

and Brdu incorporation, whereas miR-377 over-expression further significantly increased the cell viability and Brdu incorporation. PCNA and Ki-67 were two important markers of proliferation. Therefore, we also investigated the mRNA and protein levels of PCNA and Ki-67 in this study. As shown in Fig. 1c–f, miR-377 knockdown significantly reduced the high glucose and hypoxia-induced the mRNA and protein levels of PCNA and Ki-67, whereas miR-377 over-expression further significantly increased the mRNA and protein levels of PCNA and Ki-67.

Cell proliferation was accomplished by the cell cycle progression and transition [26]. Cell cycle distribution was evaluated by PI staining to assess the effect of miR-377 on cell cycle progression and transition. As shown in Fig. 2a, b, miR-377 knockdown significantly suppressed the high glucose and hypoxia-induced proportion of cells in S phase and G2/M phase, enhanced the high glucose and hypoxia-induced proportion of cells in G0/G1 phase; on the contrary, miR-377 over-expression further significantly enhanced the high glucose and hypoxia-induced proportion of cells in S phase and G2/M phase, suppressed the high glucose and hypoxia-induced proportion of cells in G0/G1 phase. We further investigated the mRNA and protein levels of cyclinD1 and cyclinB in this study. As shown in Fig. 2c–f, miR-377 knockdown significantly reduced the high glucose and hypoxia-induced the mRNA and protein levels of cyclinD1 and cyclinB, whereas miR-377 over-expression further significantly increased the mRNA and protein levels of cyclinD1 and cyclinB.

These data suggested that down-regulation of miR-377 could suppress high glucose and hypoxia-induced proliferation and cell cycle progression in HRECs.

Effect of miR-377 on high glucose and hypoxia-induced migration and angiogenesis in HRECs

Cell migration is a key step in angiogenesis of DR [27]. High glucose and hypoxia could increase the migration of HRECs (Fig. 3a–d). To investigate whether miR-377 was capable of affecting the ability of migration under the high glucose and hypoxia condition in HRECs, miR-377 knockdown or miR-377 over-expression was employed in this study. The ability of cell migration was detected by wound healing assay and transwell assay. As shown in Fig. 3a–d, miR-377 knockdown significantly suppressed the ability of cell migration induced by high glucose and hypoxia, however, miR-377 over-expression further significantly promoted the ability of cell migration induced by high glucose and hypoxia. We further investigated the mRNA and protein levels of MMP-2 and MMP-9 in this study. As shown in Fig. 3e–h, miR-377 knockdown significantly reduced the high glucose and hypoxia-induced the mRNA and protein levels
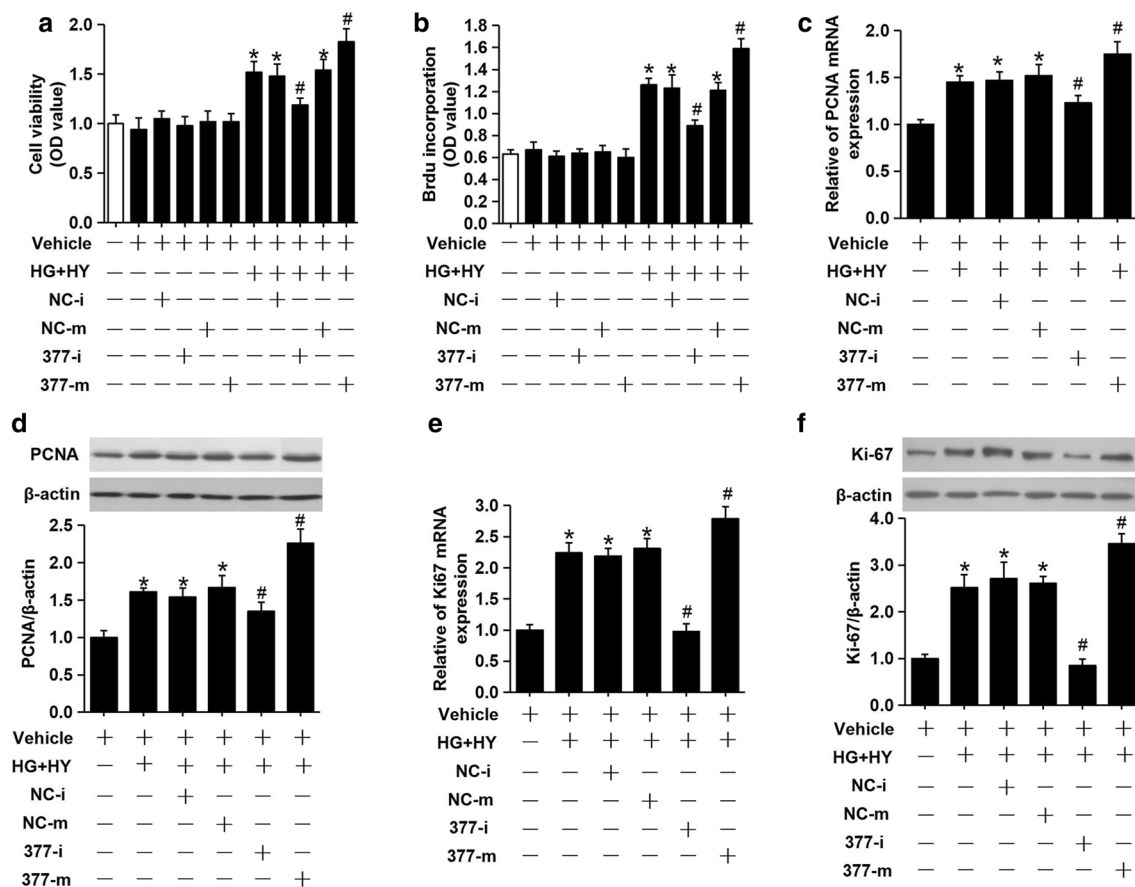
Fig. 1 Effect of miR-377 on proliferation induced by high glucose and hypoxia in HRECs. HRECs were treated with high glucose and hypoxia (27.5 mmol/L D-glucose + 150.0 μmol/L CoCl₂) for 48 h after transfection with miR-377 inhibitor or miR-377 mimic. **a** The cell viability was measured by CCK-8 assay. **b** The Brdu incorporation was measured by Brdu colorimetric assay. **c, d** The mRNA and protein levels of PCNA were detected by qRT-PCR and Western blot, respectively; **c** the mRNA level of PCNA, **d** the protein level of PCNA. **e, f** The mRNA and protein levels of Ki-67 were detected by qRT-PCR and Western blot, respectively; **e** the mRNA level of Ki-67, **f** the protein level of Ki-67. Vehicle: DMSO; *HG + HY* high glucose and hypoxia, *NC-i* negative control miR inhibitor, *NC-m* negative control miR mimic, *377-m* miR-377 mimic, *377-i* miR-377 inhibitor. All data are presented as mean ± SD, $n = 3$ in each group. *$P < 0.05$ vs. vehicle group; #$P < 0.05$ vs. vehicle + HG + HY group

of MMP-2 and MMP-9, whereas miR-377 over-expression further significantly increased the mRNA and protein levels of MMP-2 and MMP-9. We also investigated the MMP inhibitors (Batimastat and Ilomastat) on the high glucose and hypoxia-induced migration in HRECs. As shown in Supplemental Fig. 4, cell migration was inhibited after Batimastat or Ilomastat pre-treatment prior to high glucose and hypoxia stimulation.

HRECs were plated on Matrigel form tubular structures to simulate the angiogenesis procedure. As shown in Fig. 4a, b, miR-377 knockdown significantly reduced the formation of capillary-like structures on the Matrigel induced by high glucose and hypoxia, however, miR-377 over-expression further significantly increased the formation of capillary-like structures on the Matrigel induced by high glucose and hypoxia. VEGF was a key molecule of angiogenesis. We further investigated the mRNA and protein levels of VEGF

in this study. As shown in Fig. 4c, d, miR-377 knockdown significantly reduced the high glucose and hypoxia-induced the mRNA and protein levels of VEGF, whereas miR-377 over-expression further significantly increased the mRNA and protein levels of VEGF. These data suggested that down-regulation of miR-377 could suppress high glucose and hypoxia-induced angiogenesis in HRECs.

Effect of miR-377 on high glucose and hypoxia induced the secretion of pro-inflammatory cytokines in HRECs

Inflammatory response throughout the development of DR [28]. The release of TNF-α, IL-8, IL-6 and MCP-1 was evaluated by ELISA assay. As shown in Fig. 5a–d, miR-377 knockdown significantly reduced the pro-inflammatory cytokines release induced by high glucose and hypoxia,
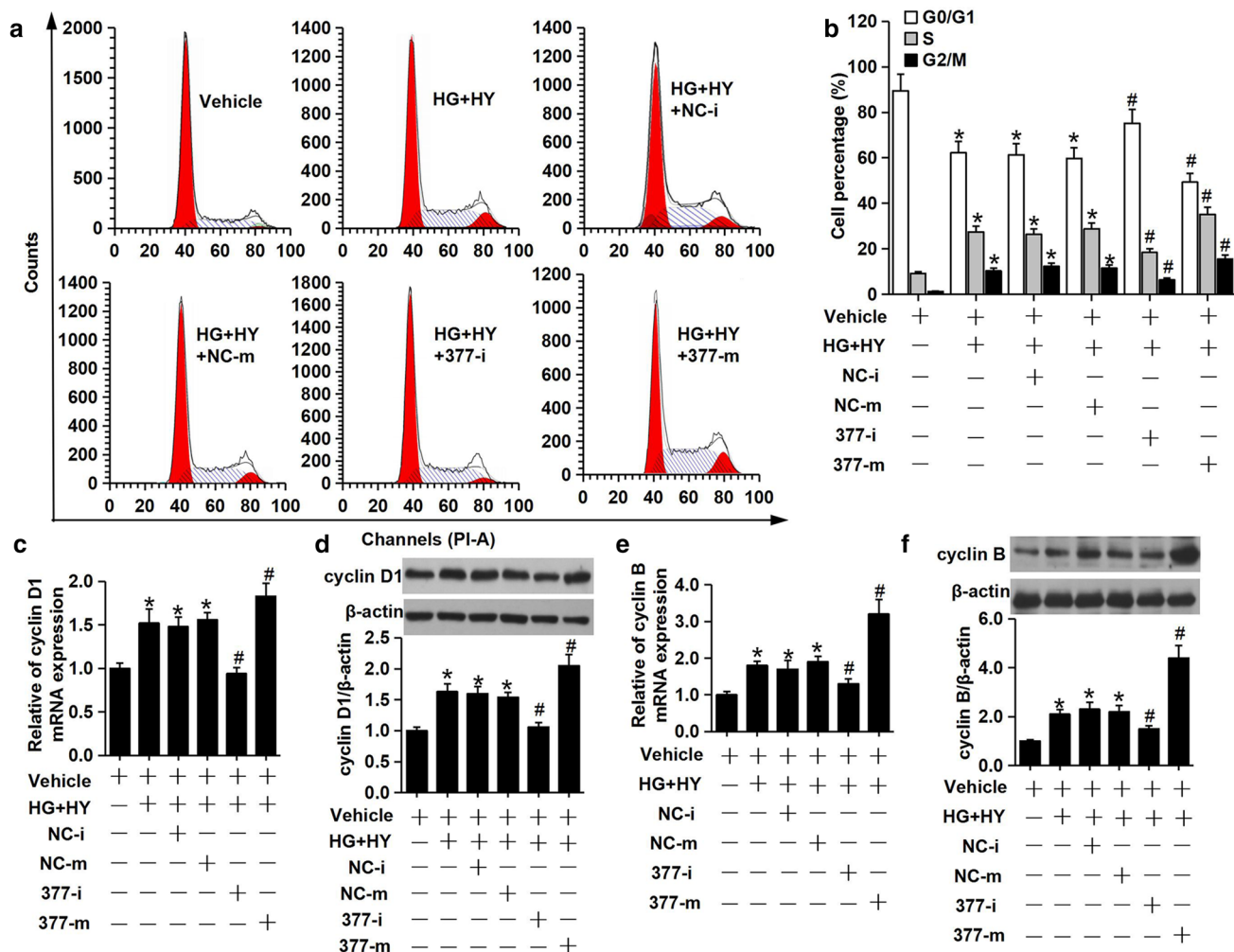
Fig. 2 Effect of miR-377 on cell cycle transition induced by high glucose and hypoxia in HRECs. HRECs were treated with high glucose and hypoxia (27.5 mmol/L D-glucose + 150.0 μmol/L CoCl$_2$) for 48 h after transfection with miR-377 inhibitor or miR-377 mimic. **a, b** Cell cycle distribution was evaluated by PI staining using a flow cytometry; **a** representative images of PI staining, **b** quantification results of cell cycle distribution. **c, d** The mRNA and protein levels of cyclinD1 were detected by qRT-PCR and Western blot, respectively; **c** the mRNA level of cyclinD1, **d** the protein level of cyclinD1. **e, f** The mRNA and protein levels of cyclinB were detected by qRT-PCR and Western blot, respectively; **e** the mRNA level of cyclinB, **d** the protein level of cyclinB. Vehicle: DMSO; *HG + HY* high glucose and hypoxia, *NC-i* negative control miR inhibitor, *NC-m* negative control miR mimic, *377-m* miR-377 mimic, *377-i* miR-377 inhibitor. All data are presented as mean ± SD, $n = 3$ in each group. $*P < 0.05$ vs. vehicle group; $^{\#}P < 0.05$ vs. vehicle + HG + HY group

however, miR-377 over-expression further significantly increased the pro-inflammatory cytokines release induced by high glucose and hypoxia.
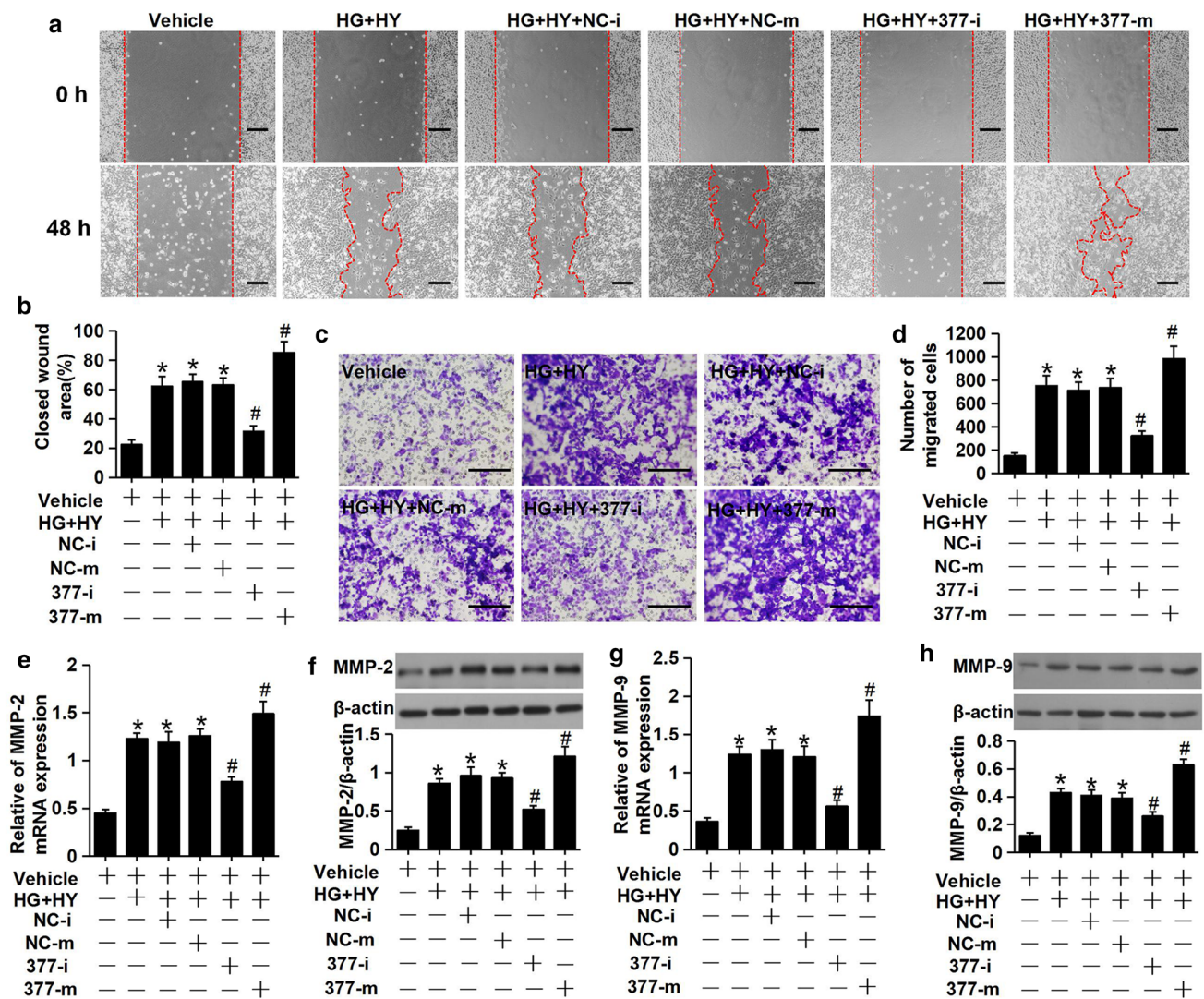
Effect of miR-377 on high glucose and hypoxia-induced the activation of NF-κB signaling pathway in HRECs

NF-κB pathway has been widely reported to be a responsible for transduction of signaling to trigger cell proliferation [29], cell cycle transition [30], cell migration [31], angiogenesis [32] and the pro-inflammatory cytokines release [33]. In the study, we found that miR-377 knockdown significantly inhibited high glucose and hypoxia-induced the protein expressions of p-IκBα (Fig. 6a), p-P65 (Fig. 6b) and nuclear P65 (Fig. 6c, d), however, miR-377 over-expression further significantly promoted high glucose and hypoxia-induced the protein expressions of p-IκBα (Fig. 6a), p-P65 (Fig. 6b) and nuclear P65(Fig. 6c, d).

SIRT1 is a direct target gene of miR-377

Using online databases including TargetScanHuman 7.2 and miRanda, we found that SIRT1 was a binding target gene of miR-377(Fig. 7c). Then, we employed qRT-PCR and Western blot to explore the mRNA and protein levels
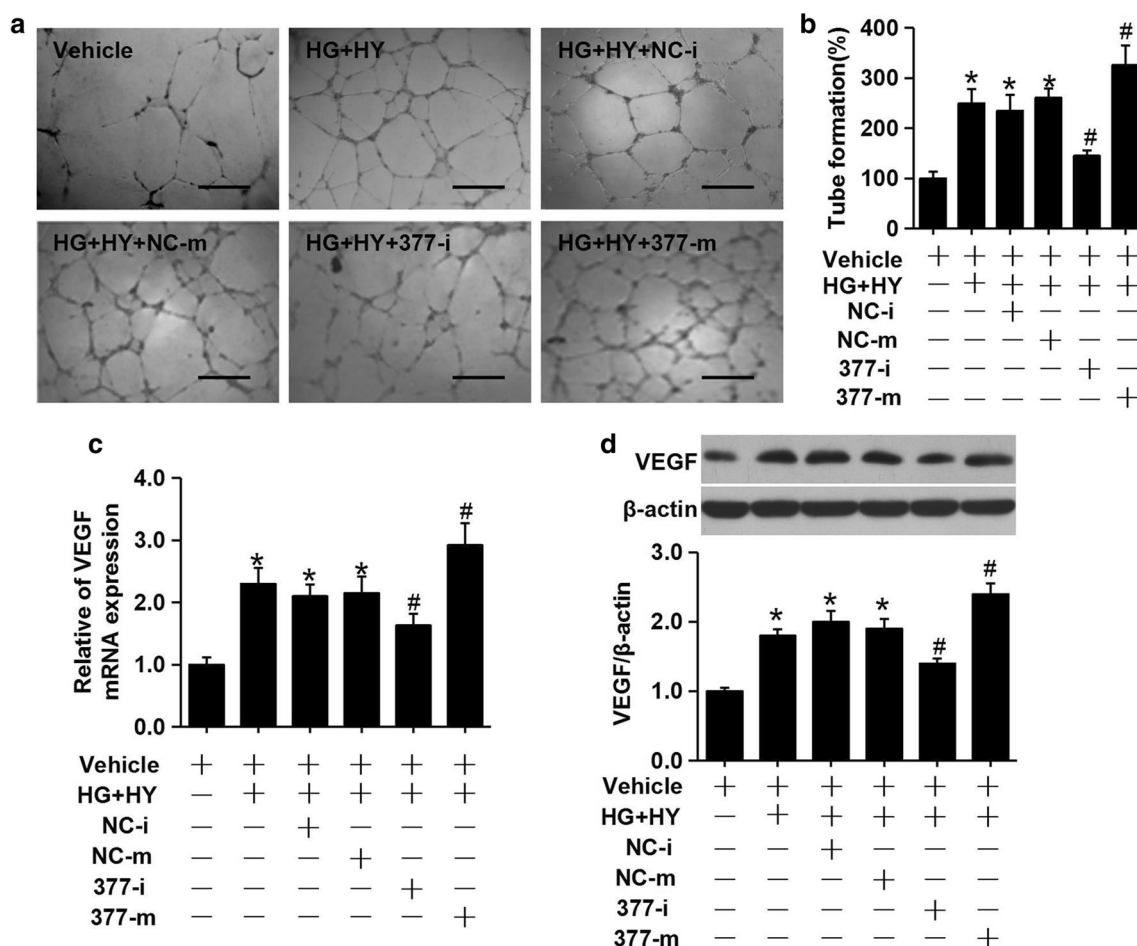
Fig. 3 Effect of miR-377 on cell migration induced by high glucose and hypoxia in HRECs. HRECs were treated with high glucose and hypoxia (27.5 mmol/L D-glucose + 150.0 μmol/L CoCl₂) for 48 h after transfection with miR-377 inhibitor or miR-377 mimic. **a, b** Cell migration was evaluated by wound healing assay; **a** representative images of wound healing assay, **b** quantification results of closed wound area. **c, d** Cell migration was evaluated by transwell assay; **c** representative images of transwell assay, **d** quantification results of number of migrated cells. **e, f** The mRNA and protein levels of MMP-2 were detected by qRT-PCR and Western blot, respectively;

e the mRNA level of MMP-2, **f** the protein level of MMP-2. **g, h** The mRNA and protein levels of MMP-9 were detected by qRT-PCR and Western blot, respectively; **g** the mRNA level of MMP-9, **h** the protein level of MMP-9. Vehicle: DMSO; *HG + HY* high glucose and hypoxia, *NC-i* negative control miR inhibitor, *NC-m* negative control miR mimic, *377-m* miR-377 mimic, *377-i* miR-377 inhibitor. Scale bar = 100 μm. All data are presented as mean ± SD, $n = 3$ in each group. *$P < 0.05$ vs. vehicle group; #$P < 0.05$ vs. vehicle + HG + HY group

induced by high glucose and hypoxia. We found that both the mRNA and protein expressions of SIRT1 were significantly decreased (Supplemental Fig. 2D–F, Fig. 7a, b). Next, we investigated whether miR-377 knockdown or over-expression was capable of affecting the mRNA and protein levels of SIRT1 under the high glucose and hypoxia condition in HRECs. As shown in Fig. 7a, b, miR-377 knockdown further significantly promoted the mRNA and protein levels of SIRT1 induced by high glucose and hypoxia, however, miR-377 over-expression significantly inhibited the mRNA

and protein levels of SIRT1 induced by high glucose and hypoxia. To further confirm whether miR-377 directly target SIRT1, we cloned the SIRT1-3′UTR or mutated the putative miR-377 binding site of SIRT1-3′UTR into the luciferase reporter pGL3-control vector (Fig. 7c) and co-transfected with miR-377 mimic or inhibitor into HRECs. As shown in Fig. 7d, e, after co-transfection for 48 h, miR-377 inhibitor or mimic significantly promoted or suppressed the luciferase activity after transfection with SIRT1-3′UTR, respectively; however, the SIRT1 mutate 3′-UTR reversed the functional

Fig. 4 Effect of miR-377 on angiogenesis induced by high glucose and hypoxia in HRECs. HRECs were treated with high glucose and hypoxia (27.5 mmol/L D-glucose + 150.0 μmol/L CoCl$_2$) for 48 h after transfection with miR-377 inhibitor or miR-377 mimic. **a, b** Angiogenesis was evaluated by tubular formation assay; **a** Representative images of tube-like structures, **b** quantification results of tubular formation. **c, d** The mRNA and protein levels of VEGF were detected by qRT-PCR and Western blot, respectively; **c** the mRNA level of VEGF, **d** the protein level of VEGF. Vehicle: DMSO; *HG + HY* high glucose and hypoxia, *NC-i* negative control miR inhibitor, *NC-m* negative control miR mimic, *377-m* miR-377 mimic, *377-i* miR-377 inhibitor. Scale bar = 100 μm. All data are presented as mean ± SD, $n = 3$ in each group. *$P < 0.05$ vs. vehicle group; #$P < 0.05$ vs. vehicle + HG + HY group

roles of miR-377. The data suggested that miR-377 could negatively regulate SIRT1.

Altered SIRT1 expression to simulate the functional roles of miR-377

To investigate the effect of SIRT1 on high glucose and hypoxia-induced cell proliferation, cell migration, angiogenesis, the pro-inflammatory cytokines release and the activation of NF-κB signaling pathway in HRECs, we transfected the cells with si-SIRT1 or pcDNA3.1-SIRT1. As shown in Fig. 8, SIRT1 knockdown by transfected with si-SIRT1 (Fig. 8a) increased the cell viability (Fig. 8b), Brdu incorporation (Fig. 8c), cell migration (Fig. 8d), angiogenesis (Fig. 8e), TNF-α release (Fig. 8f), IL-8 release (Fig. 8g), IL-6 release (Fig. 8h), and the protein level of p-P65 (Fig. 8j)

induced by high glucose and hypoxia; However, SIRT1 over-expression by transfected with pcDNA3.1-SIRT1 (Fig. 8a) decreased the cell viability (Fig. 8b), Brdu incorporation (Fig. 8c), cell migration (Fig. 8d), angiogenesis (Fig. 8e), TNF-α release (Fig. 8f), IL-8 release (Fig. 8g), IL-6 release (Fig. 8h), and the protein level of p-P65 (Fig. 8j) induced by high glucose and hypoxia. SIRT1 knockdown promoted the protein levels of VEGF, PCNA, Ki-67, MMP-2 and MMP-9 under the high glucose and hypoxia condition in HRECs, However, SIRT1 over-expression inhibited the protein levels of VEGF, PCNA, Ki-67, MMP-2 and MMP-9 under the high glucose and hypoxia condition in HRECs (Fig. 8i). Furthermore, over-expression of SIRT1 by transfected with pcDNA3.1-SIRT1 significantly reversed the inhibitory effects of miR-377 inhibitor on HG + HY-induced cell viability, Brdu incorporation, cell migration, angiogenesis,

Fig. 5 Effect of miR-377 on pro-inflammatory cytokines release induced by high glucose and hypoxia in HRECs. HRECs were treated with high glucose and hypoxia (27.5 mmol/L D-glucose + 150.0 μmol/L CoCl$_2$) for 48 h after transfection with miR-377 inhibitor or miR-377 mimic. **a–d** The levels of pro-inflammatory cytokines were evaluated by ELISA assay; **a** the level of TNF-α, **b** the level of IL-8, **c** the level of IL-6, **d** the level of MCP-1. Vehicle: DMSO; *HG + HY* high glucose and hypoxia, *NC-i* negative control miR inhibitor, *NC-m* negative control miR mimic, *377-m* miR-377 mimic, *377-i* miR-377 inhibitor. All data are presented as mean ± SD, n = 3 in each group. *$P < 0.05$ vs. vehicle group; #$P < 0.05$ vs. vehicle + HG + HY group
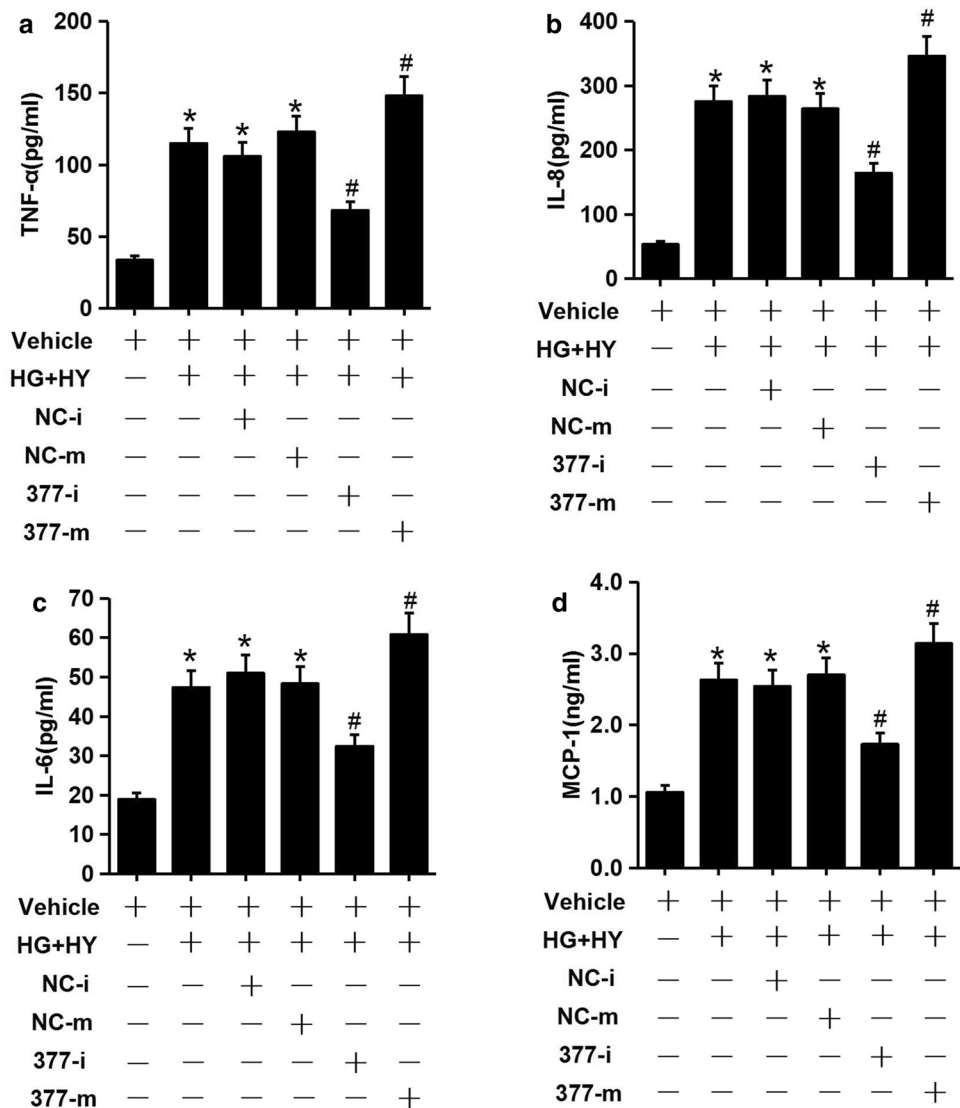

secretions of pro-inflammatory cytokine and the protein level of p-P65 (Supplemental Fig. 5A); Contrary, SIRT1 knockdown by transfected with si-SIRT1 reversed the promotive effects of miR-377 mimic on HG + HY-induced cell viability, Brdu incorporation, cell migration, angiogenesis, secretions of pro-inflammatory cytokine and the protein level of p-P65 (Supplemental Fig. 5B). These data confirmed that SIRT1 had a opposite function to miR-377 under the high glucose and hypoxia condition in HRECs.

Discussion

Diabetic retinopathy (DR), one of the most common microvascular complications of diabetes, is a chronic progressive eye disease with complex pathogenesis [2]. Although many researchers have made a lot of experimental results on DR, the exact pathogenesis is still unclear. Neovascularization on the surface of the retina is an essential process of proliferative DR [8]. Moreover, in recent years, more and more interest in the functional role of miRNAs in regulation of angiogenesis [34, 35]. Moreover, in this study, we used high glucose and hypoxia-mimetic agent to simulate the diabetic retinopathy milieu in HRECs and further to explore the role of miR-377 in regulation of angiogenesis in DR. The results showed that high glucose and hypoxia stimulation can significantly promote angiogenic functions including cell viability, cell proliferation, cell cycle transition, cell migration and angiogenesis and at the same time, the higher expression of miR-377 can be detected in this process. We further altered the miR-377 expression by transfected with miR-377 inhibitor or miR-377 mimic in HRECs, and investigated the regulatory effects of miR-377 on the perspective of the angiogenic functions. MiR-377 knockdown significantly suppressed the angiogenic functions, however, miR-377 over-expression further significantly promoted the

Fig. 6 Effect of miR-377 on activation of NF-κB signaling pathway induced by high glucose and hypoxia in HRECs. HRECs were treated with high glucose and hypoxia (27.5 mmol/L D-glucose + 150.0 μmol/L CoCl$_2$) for 48 h after transfection with miR-377 inhibitor or miR-377 mimic. **a–d** The activation of NF-κB pathway was measured by Western blot assay; **a** the protein level of p-IκBα, **b** the protein level of p-P65, **c, d** the protein levels of nuclear P65 and cytosolic P65. Vehicle: DMSO; *HG + HY* high glucose and hypoxia, *NC-i* negative control miR inhibitor, *NC-m* negative control miR mimic, *377-m* miR-377 mimic, *377-i* miR-377 inhibitor. All data are presented as mean ± SD, n = 3 in each group. *P < 0.05 vs. vehicle group; #P < 0.05 vs. vehicle + HG + HY group
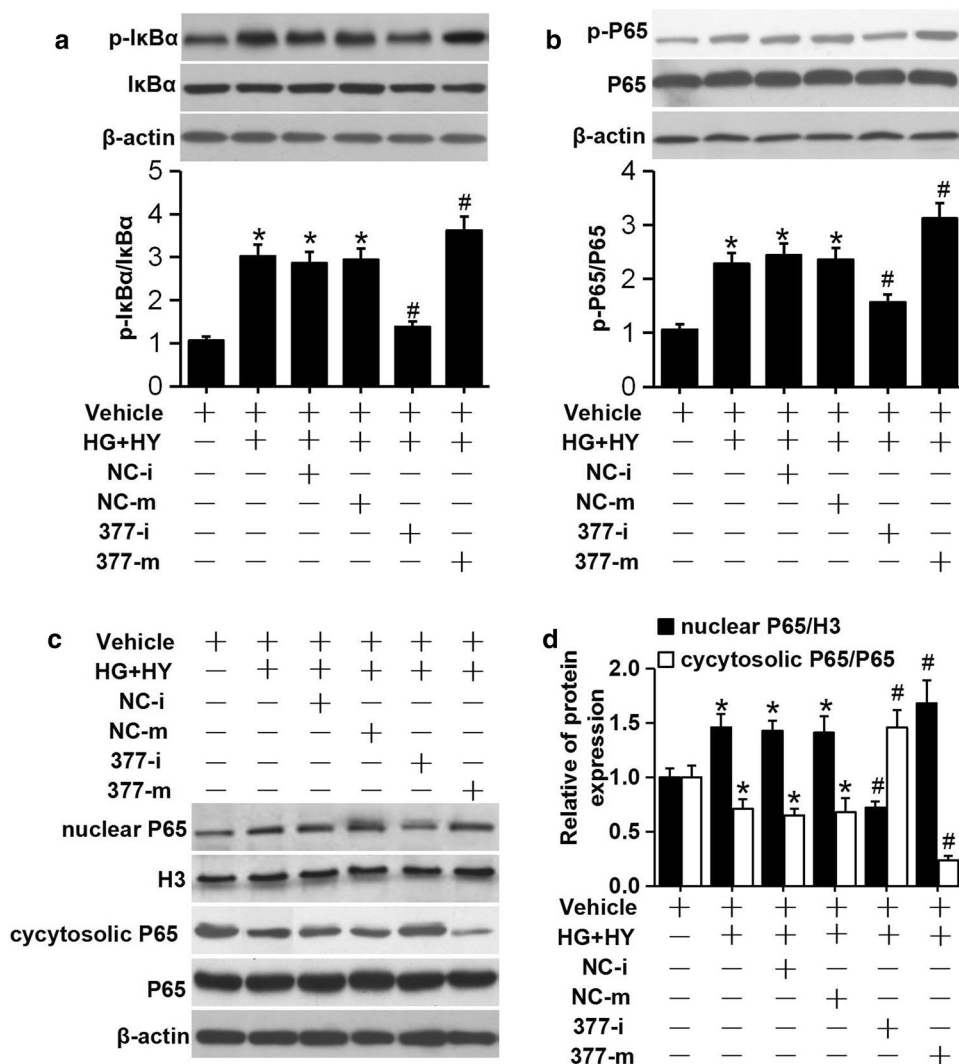

angiogenic functions under high glucose and hypoxia condition. The results confirmed that miR-377 could be involved in the regulation of the angiogenic functions of HRECs under high glucose and hypoxia condition.

Long-term chronic hyperglycemic and hypoxic microenvironment induced retinal endothelial cell inflammation also play a crucial role in the development of DR [36, 37]. As reported, the presence of inflammatory cells was found in the early stage of DR [36]. Moreover, with the development of DR, continuous hyperglycemic and hypoxic microenvironment induced excessive persistent inflammatory mediators accelerated DR progress [37]. In the study, we also investigated the regulatory effect of miR-377 on high glucose and hypoxia-induced the secretion of pro-inflammatory cytokines in HRECs. We have found that down-regulation of miR-377 was sufficient to inhibit high glucose and hypoxia-stimulated pro-inflammatory cytokines release in HRECs, suggesting that it was a main regulator in inflammatory response of DR. On the contrary, up-regulation of miR-377

could significantly increase pro-inflammatory cytokine release under HRECs by high glucose and hypoxia stimulation. Our data suggested that miR-377 is involved in regulation of the inflammatory response in DR progression.

As a transcription factor, NF-κB is a hub in many signal pathways and has various biological activities [29–33]. A large number of studies have suggested that the NF-κB signaling pathway is a key regulatory point for the expression of various immune-inflammatory related genes, cell proliferation, cell cycle transition, cell migration and angiogenesis in HRECs, and is involved in the occurrence and development of DR [38]. Therefore, the activity of NF-κB signaling pathway in HRECs was further examined under high glucose and hypoxia condition. The results showed that the phosphorylation of IκB and the nuclear translocation of NF-κB p65 subunits were significantly increased in HRECs under high glucose and hypoxia condition, suggesting the activation of NF-κB. We further investigated the regulatory effect of miR-377 on the high glucose and hypoxia-induced the
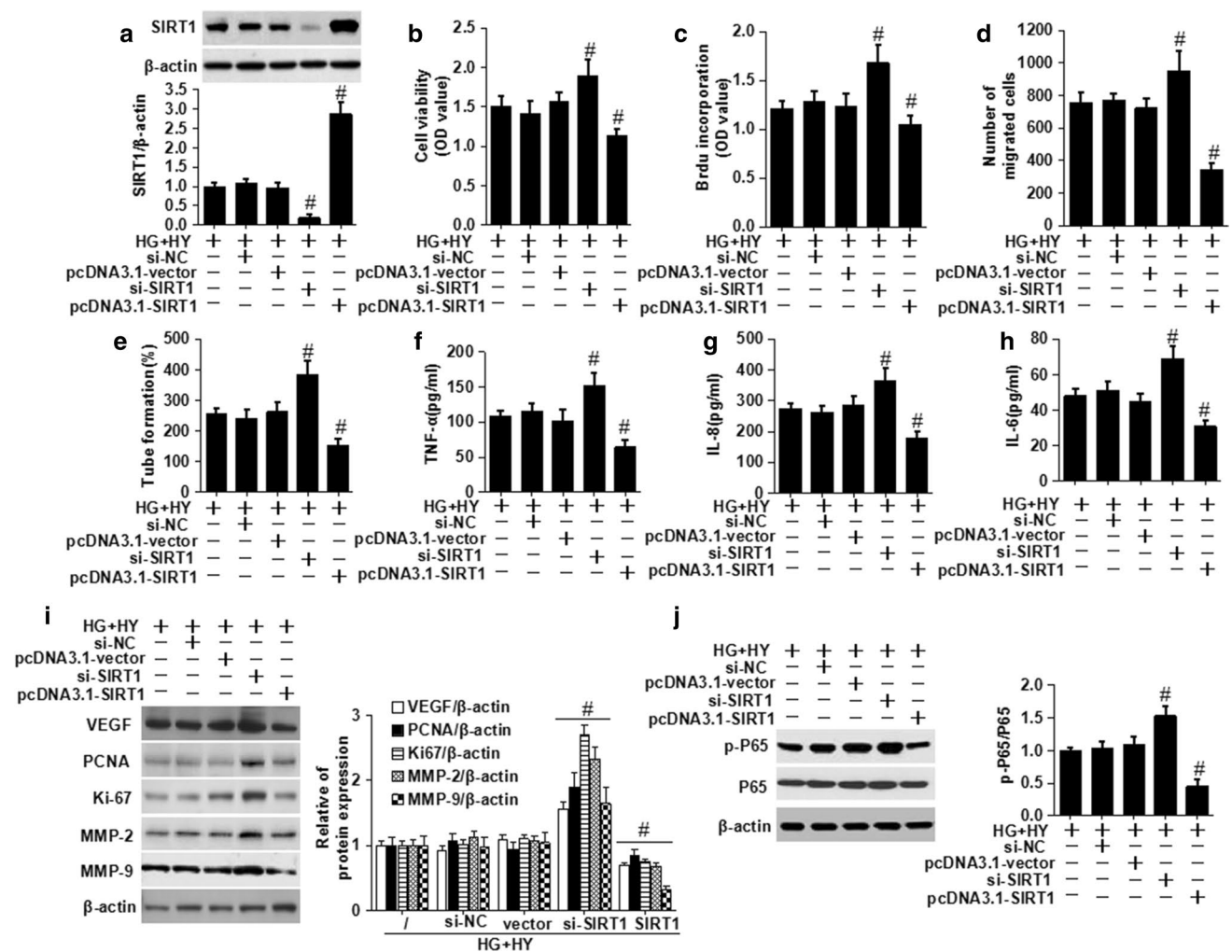
Fig. 7 SIRT1 is a direct target of miR-377. **a, b** HRECs were treated with high glucose and hypoxia (27.5 mmol/L D-glucose + 150.0 μmol/L CoCl$_2$) for 48 h after transfection with miR-377 inhibitor or miR-377 mimic. The mRNA and protein levels of SIRT1 were detected by qRT-PCR and Western blot, respectively; **a** the mRNA level of SIRT1, **b** the protein level of SIRT1. All data are presented as mean ± SD, $n=3$ in each group. *$P<0.05$ vs. vehicle group; #$P<0.05$ vs. vehicle + HG + HY group. **c** The predicted binding site of miR-377 in the 3′-UTR of SIRT1. **d, e** The relative luciferase activities of the binding site of SIRT1 were detected by dual-luciferase reporter assay; **d** HRECs were co-transfected with miR-377 inhibitor and pGL3-SIRT1-WT or pGL3-SIRT1-MUT, **e** HRECs were co-transfected with miR-377 mimic and pGL3-SIRT1-WT or pGL3-SIRT1-MUT. Vehicle: DMSO; *HG + HY* high glucose and hypoxia, *NC-i* negative control miR inhibitor, *NC-m* negative control miR mimic, *377-m* miR-377 mimic, *377-i* miR-377 inhibitor. All data are presented as mean ± SD, $n=3$ in each group. *$P<0.05$ vs. pGL3-SIRT1-WT group
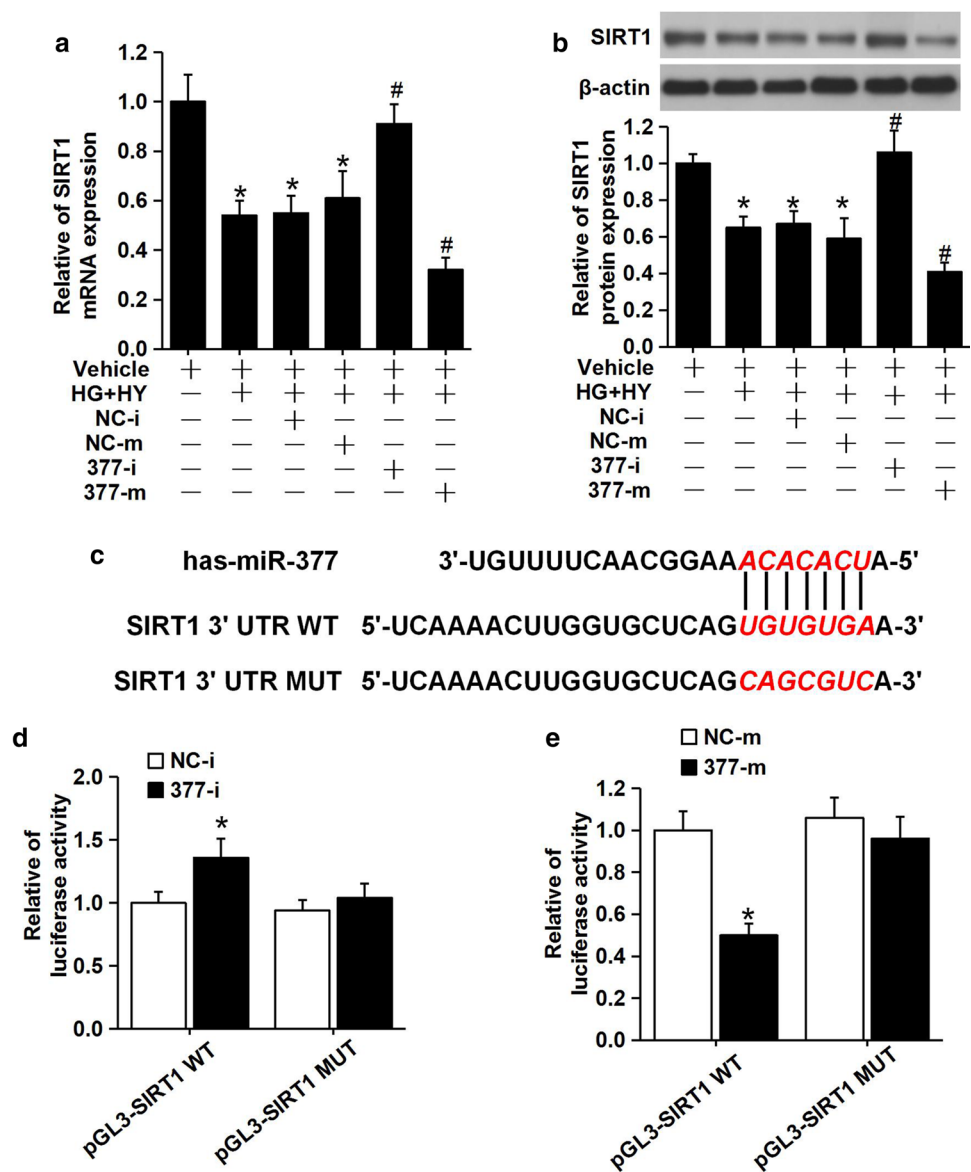
activation of NF-κB. We found that the activity of NF-κB in HRECs was inhibited after transfection with miR-377 inhibitor, on the contrary, the activity of NF-κB in HRECs was further activated after transfection with miR-377 mimic. The results confirmed the correlation between the NF-κB signaling pathway and the pathological changes of HRECs induced by high glucose and hypoxia. Meanwhile, miR-377 could affect the activity of NF-κB pathway, which may be one of the signaling pathways that miR-377 was involved in regulating the inflammatory response and angiogenesis of HRECs.

MiRNA exerts biological effects through target genes [10]. We also demonstrated that specifically targeted SIRT1 could attenuate high glucose and hypoxia-induced angiogenic functions and pro-inflammatory cytokine release in HRECs. SIRT1 depends on deacetylase to transfer the acetyl from the protein, and is closely related to DR [39, 40]. As reported, hyperglycemia reduces intercellular NAD$^+$ and decreases SIRT1 expression, and SIRT1 can inhibit the transcription of NF-kB gene by directly acetylating Rela/P65 protein lysine site 310 [39]. In addition, SIRT1 regulates the retinal microangiogenesis and the secretion of inflammatory factors induced by high glucose or hypoxia [40]. Consistent with previous studies [39, 40], our data suggested that SIRT1 was considered as an important target for treatment of DR. Moreover, we further proved that the effects of SIRT1 on angiogenic functions can be attributed to its regulation of important downstream factors such as PCNA, Ki-67, MMP-2, MMP-9 and VEGF, thus linking NF-kB pathway that eventually contribute to these alterations. In this study, our data confirmed that SIRT1 had a opposite function to miR-377

Fig. 8 Effect of SIRT1 on the angiogenic functions, the pro-inflammatory cytokine release and the activation of NF-κB signaling pathway induced by high glucose and hypoxia in HRECs. HRECs were treated with high glucose and hypoxia (27.5 mmol/L D-glucose + 150.0 μmol/L CoCl$_2$) for 48 h after transfection with si-SIRT1 or pcDNA3.1-SIRT1. **a** The transfection efficiency was measured by Western blot assay. **b** The cell viability was measured by CCK-8 assay. **c** The Brdu incorporation was measured by Brdu colorimetric assay. **d** Cell migration was evaluated by transwell assay. **e** Angiogen-esis was evaluated by tubular formation assay. **f–h** The levels of pro-inflammatory cytokines were evaluated by ELISA assay; **f** the level of TNF-α, **g** the level of IL-8, **h** the level of IL-6. **i** The protein levels of VEGF, PCNA, Ki-67, MMP-2 and MMP-9 were detected by Western blot assay. **j** The protein levels of p-P65 was detected by Western blot assay. Vehicle: DMSO; *HG + HY* high glucose and hypoxia. All data are presented as mean ± SD, *n* = 3 in each group. #*P* < 0.05 vs. HG + HY alone group

under the high glucose and hypoxia condition in HRECs and confirmed that miR-377 directly targeted SIRT1 to affect high glucose and hypoxia-stimulated the NF-kB pathway transmission and to modulate angiogenic functions and pro-inflammatory cytokines release in HRECs cells. Collectively, our results confirmed an inverse regulatory relationship between SIRT1 and miR-377 in HRECs.

In conclusion, our data proved that down-regulation of miR-377 preventing high glucose and hypoxia-induced angiogenesis and inflammation by direct up-regulation of target gene SIRT1 expression in HRECs.

Compliance with ethical standards

Conflict of interest The authors have declared that no competing interests exist.

References

1. Chan JC, Zhang Y, Ning G. Diabetes in China: a societal solution for a personal challenge. Lancet Diabetes Endocrinol. 2014;2:969–79. https://doi.org/10.1016/S2213-8587(14)70144-5.
2. Muc R, Saracen A, Grabska-Liberek I. Associations of diabetic retinopathy with retinal neurodegeneration on the background of diabetes mellitus. Overview of recent medical studies with an assessment of the impact on healthcare systems. Open Med (Wars). 2018;13:130–6. https://doi.org/10.1515/med-2018-0008.
3. Dixon CJ, Knight T, Binns E, Ihaka B, O'Brien D. Clinical measures of balance in people with type two diabetes: a systematic literature review. Gait Posture. 2017;58:325–32. https://doi.org/10.1016/j.gaitpost.2017.08.022.
4. Uemura A. Pharmacologic management of diabetic retinopathy. J Biochem. 2018;163:3–9. https://doi.org/10.1093/jb/mvx057.
5. Marahrens L, Kern R, Ziemssen T, Fritsche A, Martus P, Ziemssen F, Roeck D. Patients' preferences for involvement in the decision-making process for treating diabetic retinopathy. BMC Ophthalmol. 2017;17:139. https://doi.org/10.1186/s12886-017-0526-z.
6. Yang HS, Kim JG, Cha JB, Yun YI, Park JH, Woo JE. Quantitative analysis of neural tissues around the optic disc after panretinal photocoagulation in patients with diabetic retinopathy. PLoS One. 2017;12:e0186229. https://doi.org/10.1371/journal.pone.0186229.
7. Chen Q, Tan F, Wu Y, Zhuang X, Wu C, Zhou Y, Li Y, Cheng D, Wang J, Lu F, Shen M. Characteristics of retinal structural and microvascular alterations in early type 2 diabetic patients. Invest Ophthalmol Vis Sci. 2018;59:2110–8. https://doi.org/10.1167/iovs.17-23193.
8. Shao J, Yin Y, Yin X, Ji L, Xin Y, Zou J, Yao Y. Transthyretin exerts pro-apoptotic effects in human retinal microvascular endothelial cells through a GRP78-dependent pathway in diabetic retinopathy. Cell Physiol Biochem. 2017;43:788–800. https://doi.org/10.1159/000481562.
9. Xu J, Chen LJ, Yu J, Wang HJ, Zhang F, Liu Q, Wu J. Involvement of advanced glycation end products in the pathogenesis of diabetic retinopathy. Cell Physiol Biochem. 2018;48:705–17. https://doi.org/10.1159/000491897.
10. Sethi S, Sethi S, Bluth MH. Clinical implication of microRNAs in molecular pathology: an update for 2018. Clin Lab Med. 2018;38:237–51. https://doi.org/10.1016/j.cll.2018.02.003.
11. Kong P, Chen L, Yu M, Tao J, Liu J, Wang Y, Pan H, Zhou W, Wang S. miR-3178 inhibits cell proliferation and metastasis by targeting Notch1 in triple-negative breast cancer. Cell Death Dis. 2018;9:1059. https://doi.org/10.1038/s41419-018-1091-y.
12. Gao Y, Xiao F, Wang C, Wang C, Cui P, Zhang X, Chen X. Long noncoding RNA MALAT1 promotes osterix expression to regulate osteogenic differentiation by targeting miRNA-143 in human bone marrow-derived mesenchymal stem cells. J Cell Biochem. 2018;119:6986–96. https://doi.org/10.1002/jcb.26907.
13. Nallasamy P, Chava S, Verma SS, Mishra S, Gorantla S, Coulter DW, Byrareddy SN, Batra SK, Gupta SC, Challagundla KB. PD-L1, inflammation, non-coding RNAs, and neuroblastoma: Immuno-oncology perspective. Semin Cancer Biol. 2018;52:53–65. https://doi.org/10.1016/j.semcancer.2017.11.009.
14. Li P, Liu H, Li Y, Wang Y, Zhao L, Wang H. miR-339-5p inhibits lung adenocarcinoma invasion and migration by directly targeting BCL6. Oncol Lett. 2018;16:5785–90. https://doi.org/10.3892/ol.2018.9376.
15. Fu X, He Y, Wang X, Peng D, Chen X, Li X, Wan Q. MicroRNA-16 promotes ovarian granulosa cell proliferation and suppresses apoptosis through targeting PDCD4 in polycystic ovarian syndrome. Cell Physiol Biochem. 2018;48:670–82. https://doi.org/10.1159/000491894.
16. Zhao J, Gao S, Zhu Y, Shen X. Significant role of microRNA2195p in diabetic retinopathy and its mechanism of action. Mol Med Rep. 2018;18:385–90. https://doi.org/10.3892/mmr.2018.8988.
17. Yang C, Tahiri H, Cai C, Gu M, Gagnon C, Hardy P. microRNA-181a inhibits ocular neovascularization by interfering with vascular endothelial growth factor expression. Cardiovasc Ther. 2018;36:e12329. https://doi.org/10.1111/1755-5922.12329.
18. Qiu F, Tong H, Wang Y, Tao J, Wang H, Chen L. Inhibition of miR-21-5p suppresses high glucose-induced proliferation and angiogenesis of human retinal microvascular endothelial cells by the regulation of AKT and ERK pathways via maspin. Biosci Biotechnol Biochem. 2018;82:1366–1376. https://doi.org/10.1080/09168451.2018.1459179.
19. Chakrabarti S. MicroRNA15a-A molecule modulating multiple pathologies in diabetic retinopathy. EBioMedicine. 2016;11:13–4. https://doi.org/10.1016/j.ebiom.2016.08.017.
20. Li B, Xu WW, Han L, Chan KT, Tsao SW, Lee NPY, Law S, Xu LY, Li EM, Chan KW, Qin YR, Guan XY, He QY, Cheung ALM. MicroRNA-377 suppresses initiation and progression of esophageal cancer by inhibiting CD133 and VEGF. Oncogene. 2017;36:3986–4000. https://doi.org/10.1038/onc.2017.29.
21. Wang Q, Wang Y, Minto AW, Wang J, Shi Q, Li X, Quigg RJ. MicroRNA-377 is up-regulated and can lead to increased fibronectin production in diabetic nephropathy. FASEB J. 2008;22:4126–35. https://doi.org/10.1096/fj.08-112326.
22. Ma MM, Lin CX, Liu CZ, Gao M, Sun L, Tang YB, Zhou JG, Wang GL, Guan YY. Threonine532 phosphorylation in ClC-3 channels is required for angiotensin II-induced Cl(−) current and migration in cultured vascular smooth muscle cells. Br J Pharmacol. 2016;173:529–44. https://doi.org/10.1111/bph.13385.
23. Han J, Li Y, Liu X, Zhou T, Sun H, Edwards P, Gao H, Yu FS, Qiao X. Metformin suppresses retinal angiogenesis and inflammation in vitro and in vivo. PLoS One. 2018;13:e0193031. https://doi.org/10.1371/journal.pone.0193031.
24. Yu N, Zhu KJ, Ma SJ, Tang H, Tan XN. The total flavonoids of *Clerodendrum bungei* suppress A549 cells proliferation, migration, and invasion by impacting Wnt/β-catenin signaling. World J Tradit Chin Med. 2017;3:15–20. https://doi.org/10.4103/wjtcm.wjtcm_18_17.
25. Liang LN, Tang YZ, Zhan WJ, Li J, Ma QY, Liang J. LXHY formula inhibits choroidal neovascularization development via inhibiting the recruitment and adhesion of BMCs to the retina. World J Tradit Chin Med. 2018;4:62–8. https://doi.org/10.4103/wjtcm.wjtcm_8_18.
26. Keller-Pinter A, Szabo K, Kocsis T, Deak F, Ocsovszki I, Zvara A, Puskas L, Szilak L, Dux L. Syndecan-4 influences mammalian myoblast proliferation by modulating myostatin signalling and G1/S transition. FEBS Lett. 2018;592:3139–51. https://doi.org/10.1002/1873-3468.13227.
27. Yadav UC, Srivastava SK, Ramana KV. Prevention of VEGF-induced growth and tube formation in human retinal endothelial cells by aldose reductase inhibition. J Diabetes Complicat. 2012;26:369–77. https://doi.org/10.1016/j.jdiacomp.2012.04.017.
28. Feng S, Yu H, Yu Y, Geng Y, Li D, Yang C, Lv Q, Lu L, Liu T, Li G, Yuan L. Levels of inflammatory cytokines IL-1β, IL-6, IL-8, IL-17A, and TNF-α in aqueous humour of patients with diabetic retinopathy. J Diabetes Res. 2018;2018:8546423. https://doi.org/10.1155/2018/8546423.

29. Liu S, Bertl K, Sun H, Liu ZH, Andrukhov O, Rausch-Fan X. Effect of simvastatin on the osteogenetic behavior of alveolar osteoblasts and periodontal ligament cells. Hum Cell. 2012;25:29–35. https://doi.org/10.1007/s13577-011-0028-x.

30. Ge QL, Liu SH, Ai ZH, Tao MF, Ma L, Wen SY, Dai M, Liu F, Liu HS, Jiang RZ, Xue ZW, Jiang YH, Sun XH, Hu YM, Zhao YX, Chen X, Tao Y, Zhu XL, Ding WJ, Yang BQ, Liu DD, Zhang XR, Teng YC. RelB/NF-κB links cell cycle transition and apoptosis to endometrioid adenocarcinoma tumorigenesis. Cell Death Dis. 2016;7:e2402. https://doi.org/10.1038/cddis.2016.309.

31. Ji C, Guo H, Zhang P, Kuang W, Fan Y, Wu L. AnnexinA5 promote glioma cell invasion and migration via the PI3K/Akt/NF-κB signaling pathway. J Neurooncol. 2018;138:469–78. https://doi.org/10.1007/s11060-018-2818-4.

32. Xia ZB, Meng FR, Fang YX, Wu X, Zhang CW, Liu Y, Liu D, Li GQ, Feng FB, Qiu HY. Inhibition of NF-κB signaling pathway induces apoptosis and suppresses proliferation and angiogenesis of human fibroblast-like synovial cells in rheumatoid arthritis. Medicine (Baltimore). 2018;97:e10920. https://doi.org/10.1097/MD.0000000000010920.

33. Yuan L, Wu Y, Ren X, Liu Q, Wang J, Liu X. Isoorientin attenuates lipopolysaccharide-induced pro-inflammatory responses through down-regulation of ROS-related MAPK/NF-κB signaling pathway in BV-2 microglia. Mol Cell Biochem. 2014;386:153–65. https://doi.org/10.1007/s11010-013-1854-9.

34. Merrigan SL, Kennedy BN. Vitamin D receptor agonists regulate ocular developmental angiogenesis and modulate expression of dre-miR-21 and VEGF. Br J Pharmacol. 2017;174:2636–51. https://doi.org/10.1111/bph.13875.

35. Tiwari A, Mukherjee B, Dixit M. MicroRNA key to angiogenesis regulation: MiRNA biology and therapy. Curr Cancer Drug Targets. 2018;18:266–77. https://doi.org/10.2174/1568009617666170630142725.

36. Valle ML, Dworshak J, Sharma A, Ibrahim AS, Al-Shabrawey M, Sharma S. Inhibition of interleukin-6 *trans*-signaling prevents inflammation and endothelial barrier disruption in retinal endothelial cells. Exp Eye Res. 2018;178:27–36. https://doi.org/10.1016/j.exer.2018.09.009.

37. Kanda A, Ishida S. Receptor-associated prorenin system contributes to development of inflammation and angiogenesis in proliferative diabetic retinopathy. Inflamm Regen. 2016;36:22. https://doi.org/10.1186/s41232-016-0027-0.

38. Cai Y, Li W, Tu H, Chen N, Zhong Z, Yan P, Dong J. Curcumolide reduces diabetic retinal vascular leukostasis and leakage partly via inhibition of the p38MAPK/NF-κB signaling. Bioorg Med Chem Lett. 2017;27:1835–9. https://doi.org/10.1016/j.bmcl.2017.02.045.

39. Ott C, Jacobs K, Haucke E, Navarrete Santos A, Grune T, Simm A. Role of advanced glycation end products in cellular signaling. Redox Biol. 2014;2:411–29. https://doi.org/10.1016/j.redox.2013.12.016.

40. Chang YC, Lin CW, Hsieh MC, Wu HJ, Wu WS, Wu WC, Kao YH. High mobility group B1 up-regulates angiogenic and fibrogenic factors in human retinal pigment epithelial ARPE-19 cells. Cell Signal. 2017;40:248–57. https://doi.org/10.1016/j.cellsig.2017.09.019.